Effect of fine-scale roughness on the tractions between contacting bodies

Junki Joe[a,*], M. Scaraggi[b], J. R. Barber[a]

[a] *Department of Mechanical Engineering, University of Michigan, Ann Arbor, MI 48109-2125, U.S.A.*
[b] *DII, Universitá del Salento, 73100 Monteroni-Lecce, Italy*

Abstract

Persson's theory for the elastic contact of rough surfaces is modified to include the compliance associated with an interface force law such as the Lennard-Jones law. We determine the effect of adding a small packet of waves on the probability distribution function [PDF] of the local interfacial gap (including the effect of elastic deformation). This procedure is then used iteratively to develop an algorithm for determining the PDF for a rough surface with a prescribed power spectral density. The results show that for untruncated quasi-fractal surfaces, the PDF then converges at large wavenumber, in contrast to the result when only elastic deformation is taken into account.

If the roughness is restricted to wavenumbers greater than a certain critical value, the algorithm predicts a converged relation between nominal traction and mean gap that can be regarded as a modified interfacial force law describing the influence of just the fine-scale roughness on the contact. In particular, the area under the resulting curve can be interpreted as a measure of interface energy as reduced by this roughness. The remaining macroscopic features of the surface can then be described using the JKR methodology in combination with this modified interface energy.

Keywords: Contact mechanics; surface roughness; adhesion.

*Corresponding author: jkjoe@umich.edu.

1. Introduction

Surfaces are rarely atomically smooth and numerous authors have attempted to predict the effect of surface roughness on the contact of nominally plane surfaces. Many of these theories are based on models of the roughness as a set of non-interacting microscopic asperities, following the seminal contribution of Greenwood and Williamson [1]. These theories have enjoyed considerable success in explaining the physical observation that [for example] electrical contact conductance and the frictional forces during sliding are approximately proportional to the applied normal force.

An alternative approach due to Persson [2] [see also [3, 4]] defines the function $\Phi(p)$ representing the probability that an arbitrary point on the interface should be in contact at a given pressure p, for a surface whose power spectral density [PSD] $P_S(k)$ is truncated at some upper cutoff k. An expression is then developed for the incremental change in $\Phi(p)$ due to the inclusion of an additional increment Δk of the PSD, and the effect of the entire PSD is obtained by iteration or integration. This theory is also very successful at predicting important features of the contact problem (for example, as observed in molecular and finite element simulations of particular cases [5]).

Aficionados of either theory tend to be dismissive of the claims of the other, but despite their differing approaches, the two theories often lead to surprisingly similar predictions. For example, Bush [6] used predictions of asperity heights and curvatures from profile measurements to determine parameters for an asperity model and showed that at sufficiently low nominal pressures $p_{\rm nom}$, the proportion of the nominal area $A_{\rm nom}$ in actual contact is approximated by

$$\frac{A}{A_{\rm nom}} \approx \frac{p_{\rm nom}}{E^*}\sqrt{\frac{\pi}{m_2}}\,, \tag{1}$$

where E^* is the composite elastic modulus defined by

$$\frac{1}{E^*} = \frac{(1-\nu_1)^2}{E_1} + \frac{(1-\nu_2)^2}{E_2}\,, \tag{2}$$

and m_2 is the mean square slope of the profile given by

$$m_2 = \int_{-\infty}^{\infty} k^2 P_P(k) dk = \pi \int_0^{\infty} k^3 P_S(k) dk\,, \tag{3}$$

where the profile PSD $P_P(k)$ is related to the surface PSD by

$$P_P(k) = 2\int_k^\infty \frac{sP_S(s)ds}{\sqrt{s^2-k^2}} \tag{4}$$

[7]. The corresponding prediction from Persson's theory is

$$\frac{A}{A_{\rm nom}} = \int_0^\infty \Phi(p)dp \approx \frac{2p_{\rm nom}}{E^*\sqrt{\pi m_2}}\,, \tag{5}$$

which has the same parametric dependence as (1), but a numerical multiplier differing by a factor of $2/\pi$. However, qualitative differences between the two approaches are predicted when the nominal pressure is sufficient to ensure that a significant proportion of the nominal surface is in actual contact.

1.1. Fine-scale roughness

Real surfaces often exhibit fractal character at large k, with surface PSDs of the form

$$P_S(k) = Ck^{2D-8}\,, \tag{6}$$

where C is a constant and D is the fractal dimension of the surface and lies in the range $2 < D < 3$. However, if an expression of this form is substituted into (3), the result is unbounded, so both theories predict a vanishing proportion of the nominal area in actual contact and a theoretically infinite mean contact pressure. In asperity model theories, this problem is reflected in the difficult of deciding at what scale the 'asperities' should be defined [8, 9]. Similar effects are seen in numerical studies with progressive mesh refinement [10]. Of course, fine-scale effects must ultimately be limited by plastic deformation or other failure modes of the material [11], and the continuum theory itself becomes inappropriate at length scales comparable with interatomic distances, but these arguments do not give a clear indication of the point at which $P_S(k)$ should be truncated.

1.2. Contact, separation and adhesive tractions

The difficulty with both approaches arises principally from the sharp distinction between contact and separation assumed in conventional contact mechanics. If this is relaxed through the use [say] of the Lennard-Jones traction law for contact interactions, it seems clear that the high frequency, low amplitude components of the PSD (6) will have decreasing influence on

the probability distribution function [PDF] for pressure $\Phi(p)$. By contrast, if these waves are forced into contact at zero gap, the incremental variance of contact pressure required increases without limit in proportion with the mean surface slope.

The Lennard-Jones law involves regions of tensile as well as compressive tractions and hence opens the vexed question of the influence of surface roughness on the maximum nominal tensile traction [the 'pull-off traction'] that can be supported by an interface between two otherwise plane surfaces. Fuller and Tabor [12] extended Greenwood and Williamson's model by using the 'JKR' solution [13] for each pair of interacting asperities, but the JKR theory also depends upon there being a sharp distinction between regions of contact and separation. This implies a singularity in tensile tractions at the edge of the contact region, and hence the occurrence of a finite region in which the assumed tractions exceed the theoretical strength of the materials. Tabor [14] has shown that this is an acceptable approximation for the contact of spheres only when the Tabor parameter

$$\mu = \left(\frac{R(\Delta\gamma)^2}{E^{*2}\epsilon^3} \right)^{1/3} \gg 1 \ , \tag{7}$$

where R is the radius of the sphere, $\Delta\gamma$ is the interface energy, and ϵ is a measure of the range of interatomic forces. Clearly this criterion will fail when asperities are defined at a sufficiently fine scale.

Persson and Scaraggi [15] investigated the effect of surface roughness using the so-called 'DMT' approach, in which the adhesive tractions in the separation region are estimated based on the gap that would occur in the absence of such tractions (found in this case using Persson's theory). Greenwood [16] argues that the DMT approach is not a true asymptotic solution for $\mu \ll 1$ and offers an alternative 'semi-rigid' theory in which the gap is first estimated assuming the bodies to be rigid [17], but the tractions associated with this gap are then allowed to deform the body elastically. However, this approach fails for a Gaussian rough surface, since there is then a small but finite probability of an asperity or a region of the surface having an arbitrarily large height, so two statistically rough rigid bodies could theoretically never be made to approach each other.

In this paper, we shall attempt to resolve these difficulties by developing a theory modelled on Persson's approach, but including the modulation between contact and separation associated with the Lennard-Jones law. In

particular, we shall introduce the effect of each small increment in the surface PSD using a linearized solution for the combined effect of elastic deformation and Lennard-Jones gap-dependent tractions. With this approach, we shall show that the probability distribution tends to a limit at large k, so no truncation of the PSD is necessary. The same method also allows the influence of the infinite 'tail' of the PSD on the relation between mean traction and mean gap to be estimated, suggesting a procedure for extending the JKR approach to surfaces with quasi-fractal roughness.

2. Theoretical model

We assume that the tractions σ [tensile positive] between two atomically plane surfaces are defined by the integrated Lennard-Jones law

$$\sigma(g) = \frac{8\Delta\gamma}{3\epsilon}\left(\frac{\epsilon^3}{g^3} - \frac{\epsilon^9}{g^9}\right) \tag{8}$$

[obtained through the application of the Derjaguin approach], where g is the local value of the gap (separation) between the surfaces, $\Delta\gamma$ is the interface energy and ϵ is the separation at which two unloaded bodies with plane surfaces would be in equilibrium. This relation is illustrated in Fig. 1, where σ is normalized by the maximum tensile traction [the theoretical strength]

$$\sigma_0 = \frac{16\Delta\gamma}{9\sqrt{3}\epsilon}\ , \tag{9}$$

which occurs at B, where $g = 3^{1/6}\epsilon \approx 1.201\epsilon$. The relation between ϵ and crystal lattice parameters is discussed by Yu and Polycarpou [18].

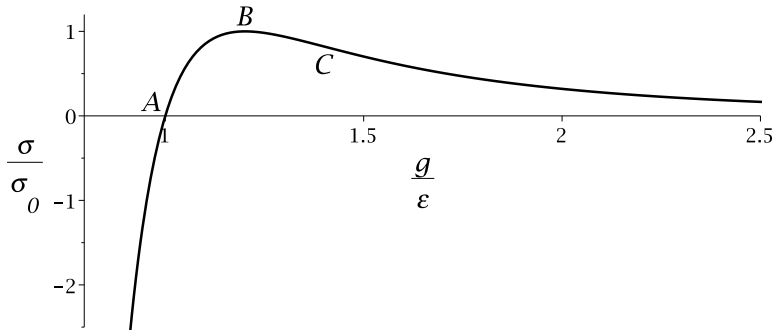

Fig. 1: The Lennard-Jones force law.

2.1. Contact problem for a single sine wave

We first consider the simpler problem in which the gap g contains a single sinusoidal wave of amplitude g_1 and wavenumber k, so that

$$g(x) = g_{\text{ave}} + g_1 \cos(kx) \ , \tag{10}$$

where g_{ave} is the mean separation.

Equation (8) and Fig. 1 define a non-linear relation, so the resulting contact pressure $p(x)$ will not be sinusoidal. However, if $g_1/\epsilon \ll 1$, we can linearize equation (8) about the mean value g_{ave}, obtaining

$$p(x) = -\sigma\left(g(x)\right) \approx \bar{p} + p_1 \cos(kx) \ , \tag{11}$$

where

$$\bar{p} = -\sigma\left(g_{\text{ave}}\right) \ ; \quad p_1 = -g_1 \left(\frac{\partial \sigma}{\partial g}\right)_{g=g_{\text{ave}}} \ . \tag{12}$$

The sinusoidal component will produce normal elastic displacements

$$u(x) = u_1 \cos(kx) \quad \text{where} \quad u_1 = \frac{2p_1}{E^* k} \tag{13}$$

(Johnson, 1985) and these increase the final gap $g(x)$, so we conclude that the original undeformed surface must have contained a sinusoidal perturbation of amplitude $h_1 = g_1 - u_1$. Using (8) to evaluate the derivative in (12), we obtain

$$g_1 = f(\tilde{g}, \tilde{k}) h_1 \quad \text{where} \quad f(\tilde{g}, \tilde{k}) = \left[1 + \frac{1}{\tilde{k}} \left(\frac{9}{\tilde{g}^{10}} - \frac{3}{\tilde{g}^4}\right)\right]^{-1} \tag{14}$$

and we have introduced the dimensionless parameters

$$\tilde{g} = \frac{g}{\epsilon} \ ; \quad \tilde{k} = \frac{3\epsilon^2 E^* k}{16 \Delta\gamma} \equiv \chi k \ ; \quad \tilde{P}_S(\tilde{k}) = \frac{P_S(k)}{\epsilon^2 \chi^2} \ . \tag{15}$$

Notice that the dimensionless wavenumber has obvious similarities to the Tabor parameter of equation (7) and we could define an equivalent Tabor parameter using the radius of the peaks of the sine wave for R. It is also worth remarking that for the contact of similar materials, the slope of the Lennard-Jones relation (8) at the equilibrium point A in Fig. 1 is related to the elastic modulus E [19]. For this case, if $\nu = 0$, the dimensionless wavenumber $\tilde{k} \approx 3k\epsilon$.

2.2. A 'small' packet of uncorrelated sine waves

We next consider the case where the surfaces are nominally plane with constant separation $\tilde{g}_0$, and we add an isotropic packet of uncorrelated sine waves whose wavenumbers lie in a band $(\tilde{k}, \tilde{k} + \Delta\tilde{k})$. If the total energy in this band is sufficiently small, the PDF of the resulting gap $\tilde{g}$ will have the Gaussian form

$$\Phi(\tilde{g}, \tilde{g}_0, \tilde{k}, \Delta\tilde{k}) = \frac{1}{\sqrt{2\pi V}} \exp\left(-\frac{(\tilde{g} - \tilde{g}_0)^2}{2V}\right) \tag{16}$$

[20], with variance

$$V(\tilde{g}_0, \tilde{k}, \Delta\tilde{k}) = 2\pi \int_{\tilde{k}}^{\tilde{k}+\Delta\tilde{k}} s\tilde{P}_S(s) f(\tilde{g}_0, s)^2 ds \ . \tag{17}$$

This argument depends on V being sufficiently small for $f(\tilde{g}, \tilde{k})$ to be considered constant in the range where $\Phi(\tilde{g})$ is not negligible [e.g. in $\tilde{g}_0 - 5\sqrt{V} < \tilde{g} < \tilde{g}_0 + 5\sqrt{V}$]. Intuitively, the resulting error should tend to zero as $\Delta\tilde{k} \to 0$, and we shall show in Section 3.1.1 that a corresponding numerical iterative solution for a given $\tilde{P}_S(\tilde{k})$ converges on a unique result in this limit.

2.3. Integration over an extended PSD

We interpret equation (16) as defining the *conditional* probability $\Phi(\tilde{g}|\tilde{g}_0)$ of a point at separation $\tilde{g}_0$ being at $\tilde{g}$ after the addition of the wave packet $\Delta\tilde{k}$. This involves the assumption that the conditional probability depends only on the local value of $\tilde{g}_0$ and hence is the same as would be obtained if the entire surface were at $\tilde{g}_0$. However, this is not very different from the assumption in Persson's theory [2, 4] that the conditional probability $\Phi(p|p_0)$ for contact pressure is given by the full contact solution, since this implies that it is uninfluenced by the possible [and indeed likely] nearness of regions of separation.

If the PDF of $\tilde{g}$ for the case where the surface PSD is truncated at $\tilde{k}$ is denoted by $\Phi(\tilde{g}, \tilde{k})$, we can determine the corresponding expression after the addition of the wave packet $\Delta\tilde{k}$ as

$$\Phi(\tilde{g}, \tilde{k} + \Delta\tilde{k}) = \int_0^\infty \Phi(\tilde{g}_0, \tilde{k}) \Phi(\tilde{g}|\tilde{g}_0) d\tilde{g}_0 = \int_0^\infty \frac{\Phi(\tilde{g}_0, \tilde{k})}{\sqrt{2\pi V}} \exp\left(-\frac{(\tilde{g} - \tilde{g}_0)^2}{2V}\right) d\tilde{g}_0 \ . \tag{18}$$

This relation can then be applied iteratively to determine $\Phi(\tilde{g})$ due to an extended PSD.

Notice that the theory developed here differs from that of Persson [2] in that from the beginning we track the evolution of the probability distribution $\Phi(\tilde{g})$ of the gap $\tilde{g}$, rather than that of the contact pressure p. We make this choice because the Lennard-Jones traction $\sigma = -p$, illustrated in Fig. 1, is a single-valued function of g, whereas for $0 < \sigma < \sigma_0$, g is a multi-valued function of p, so the probability $\Phi(p)$ entails some ambiguity as to which branch is in question. Almqvist *et al.* [21] developed expressions for $\Phi(g)$, but these were derived from $\Phi(p)$ using a strain energy argument, and assumed a sharp transition from contact to separation without traction.

2.4. Negative stiffness and instability

The function $f(\tilde{g}, \tilde{k})$ of equation (14) is negative for

$$\tilde{k} < \frac{3}{\tilde{g}^4} - \frac{9}{\tilde{g}^{10}} \,, \tag{19}$$

implying that a single sine wave of infinitesimal amplitude in the original profile would result in a sinusoidal gap that is 180 deg out of phase. In effect, the system exhibits negative stiffness in this range and the resulting solution would clearly be unstable. Instead we should anticipate a jump to one of two stable states that are not within an infinitesimal neighbourhood of the original perturbation.

In fact, if two *plane* surfaces of (say) square planform of side $2\pi/k$ are brought to a mean separation $\tilde{g}$ in the range defined by (19), it is energetically favourable for a sinusoidal perturbation to form spontaneously. However, the maximum value of the right-hand side of (19) occurs at $\tilde{g} = \sqrt[6]{15/2}$ and is $\tilde{k}_0 = \sqrt[3]{324/3125} \approx 0.470$, so this instability is precluded if we restrict attention to roughness spectra in the 'fine-scale' range $\tilde{k} > \tilde{k}_0$.

To place this value in perspective, we note that the (dimensional) peak radius of the sinusoid $h\sin(k_0 x)$ of amplitude h is $R = 1/hk_0^2$. If this value is used in the definition of the Tabor number (7), we obtain

$$\mu \approx 0.542 \sqrt[3]{\frac{\epsilon}{h}} \,. \tag{20}$$

Thus, k_0 can also be interpreted as the wavenumber above which the JKR methodology would be inappropriate for a single sine wave of amplitude $h \sim \epsilon$.

3. Results

We first consider the case where the PSD has the quasi-fractal form of equation (6) with lower and upper cutoff frequencies k_1, k_2 respectively. We start from the condition where the surface is plane so that the separation is everywhere constant and equal to g_{ave}, and hence $\Phi(\tilde{g}) = \delta(\tilde{g} - \tilde{g}_{\text{ave}})$, where $\delta(\cdot)$ is the Dirac delta function. We then add wave packets $\Delta\tilde{k}$ sequentially using equations (18, 17) until the entire PSD has been added.

3.1. Convergence tests

3.1.1. Choice of $\Delta\tilde{k}$

We argued in Section 2.2 that equation (16) is strictly correct only when V is 'sufficiently small', which here places a restriction on the value of $\Delta\tilde{k}$. For a given value of $\Delta\tilde{k}$, $V(\tilde{g}, \tilde{k}, \Delta\tilde{k})$ is a function of $\tilde{g}$ with the maximum value occurring at $\tilde{g}_0 = \sqrt[6]{15/2}$. We therefore anticipate that numerical convergence will be approximately characterized by the parameter $V_{\max} = V(\tilde{g}_0, \tilde{k}, \Delta\tilde{k})$

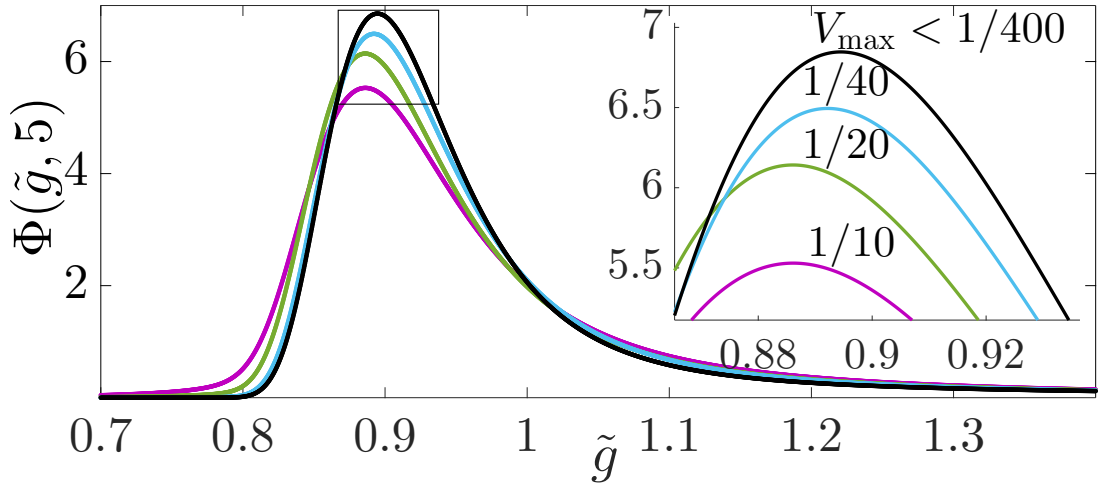

Fig. 2: Effect of maximum wave packet variance $V_{\max}$ on the convergence of the process.

Fig. 2 presents numerical calculations for the resulting PDF obtained with various values of this parameter, for the case where $\tilde{g}_{\text{ave}} = 0.98, \tilde{k}_1 = 1, \tilde{k}_2 = 5$ and the PSD is given by the dimensionless equivalent of equation

(6) with $D = 2.5$ and a multiplying constant $C = 1/\pi$. The results show that the PDF does indeed converge as $\Delta\tilde{k}$ is reduced, and the curves for values below $V_{\max} = 1/400$ are virtually indistinguishable, suggesting that this is an acceptable degree of discretization.

3.1.2. Convergence at large $\tilde{k}_2$

Fig. 3 shows results obtained for the same PSD and mean gap $\tilde{g}_{\text{ave}}$, but different values of the upper cutoff frequency $\tilde{k}_2$. Notice that there is significant evolution of the PDF as $\tilde{k}_2$ is increased, but the curves become almost identical beyond $\tilde{k}_2 = 580$, showing that the process converges as surmised in the Introduction. It follows that with this strategy, it is not necessary to impose an arbitrary truncation on the PSD.

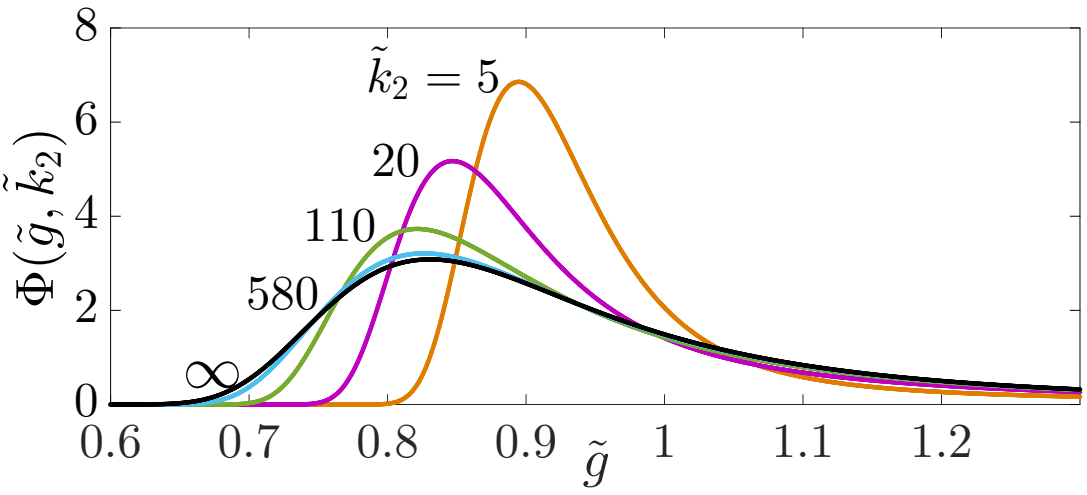

Fig. 3: Effect of upper cutoff frequency $\tilde{k}_2$ on $\Phi(\tilde{g})$.

4. Relation between mean gap and nominal traction

Once the probability distribution function $\Phi(\tilde{g})$ has been determined, the nominal (mean) traction $\bar{\sigma}$ can be obtained as

$$\bar{\sigma} = \int_0^\infty \Phi(\tilde{g})\sigma(\tilde{g})d\tilde{g} \,, \tag{21}$$

where $\sigma(\tilde{g})$ is the Lennard-Jones traction (8).

Fig. 4 shows the resulting nominal traction, normalized by the maximum Lennard-Jones tensile traction σ_0, as a function of the mean gap $\tilde{g}_{\rm ave}$, for the PSD (6) with $\tilde{k}_1 = 1, C = 1/\pi, D = 2.5$ and $\tilde{k}_2 \to \infty$. Notice that the resulting figure is qualitatively similar to that of the original L-J law of Fig. 1, but with two notable differences: (i) the maximum tensile value is significantly lower than unity, and (ii) the equilibrium point [where $\bar{\sigma} = 0$] is shifted to a value $\tilde{g}_{\rm ave} > 1$. This shift is a consequence of the high stiffness of the surface to high frequency waves. At modest nominal compressive tractions, only the peaks of the distribution come within range of L-J tractions and hence the mean planes are more separated relative to similar loading of two plane surfaces. For a given (dimensional) PSD, this mean-plane shift increases with E^* and of course would be theoretically infinite in the rigid-body (Bradley) limit [22], since the rough surface has no highest point. The modified force law of Fig. 4 preserves the $\tilde{g}_{\rm ave}^{-3}$ behaviour of the L-J law at large $\tilde{g}_{\rm ave}$, but is not of power law form in the compressive range.

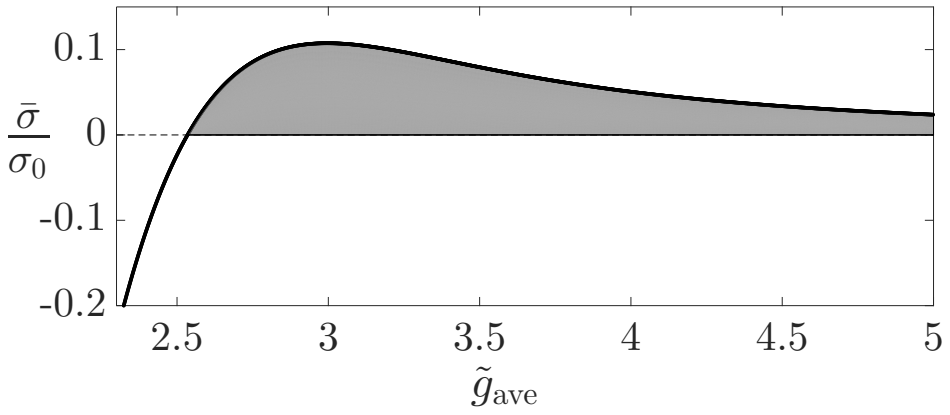

Fig. 4: Relation between mean traction $\bar{\sigma}$ and mean gap $\tilde{g}_{\rm ave}$ for $\tilde{k}_1 = 1, C = 1/\pi, D = 2.5$ and $\tilde{k}_2 \to \infty$.

The shaded area in Fig. 4 is proportional to the work that must be done per unit nominal area in order to separate the contacting rough surfaces from the equilibrium position. Thus it can be seen as a measure of interface energy $\Delta\gamma$, as modified [reduced] by the presence of fine-scale roughness $\tilde{k} > \tilde{k}_1$. Fig. 5 shows the magnitude $\Delta\gamma_{\rm eff}$ of this modified interface energy and also the maximum pull-off traction $\bar{\sigma}_{\rm max}$ as a function of the dimensionless variance of the fine-scale roughness $\tilde{m}_0 = m_0/\epsilon^2$, where

$$m_0 = 2\int_0^\infty P_P(k)dk = 2\pi\int_{k_1}^\infty kP_S(k)dk\ . \tag{22}$$

Notice that the more usual RMS roughness measure is equal to $\sqrt{m_0}$. Both $\Delta\gamma_{\text{eff}}$ and $\bar{\sigma}_{\max}$ are normalized by the plane surface values and hence tend to unity for $m_0 = 0$.

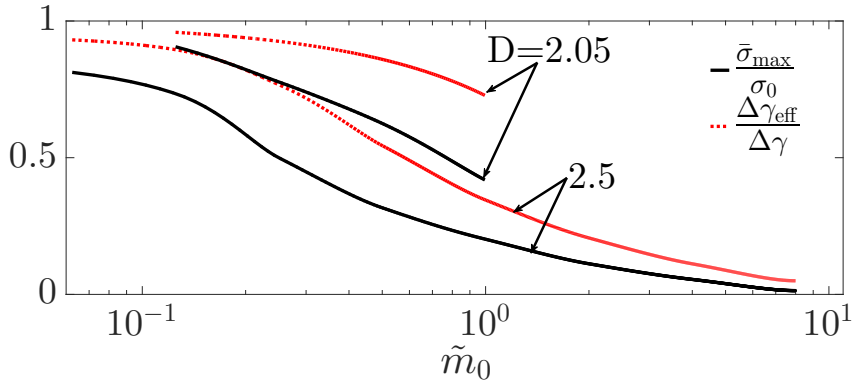

Fig. 5: Effect of fine-scale roughness on the effective interface energy $\Delta\gamma_{\text{eff}}$ and pull-off traction $\bar{\sigma}_{\max}$. Here $D = 2.05, 2.5$, $\tilde{k}_1 = 0.5$ and the height variance m_0 is changed through the constant C in (6).

Persson and Scaraggi [15] define the related quantity $\gamma_{\text{eff}}(\bar{\sigma})$ as the work done per unit area in separating two surfaces currently loaded by a mean traction $\bar{\sigma}$. They estimated it using the 'DMT' approach, in which the gap [or in this case $\Phi(g)$] is estimated based on a classical 'hard-contact' elastic model without adhesive tractions. The van der Waals' tractions associated with this gap are then summed and added to the total compressive force in the contact region to obtain the total contact force. The quantity $\Delta\gamma_{\text{eff}}$ plotted in our Fig. 5 is essentially $\gamma_{\text{eff}}(0)$. In other words, it is the work done in separating the bodies from the equilibrium position, where $\bar{\sigma} = 0$.

The results in Fig. 5 show that adhesive tractions fall off more rapidly with increasing m_0 when the fractal dimension D is larger. This is consistent with results for conventional truncated PSDs, since an increase of D at constant m_0 would then imply an increase in the surface slope variance m_2, as reported [for example] by Pastewka and Robbins [5]. Notice however that for an untruncated fractal PSD m_2 is theoretically infinite, so a criterion based on surface slopes [rather than fractal dimension] is critically dependent on the upper cutoff k_2.

5. Comparison with a discrete numerical model

In order to assess the effect of the approximations inherent in the solution, we compared the results in particular cases with the numerical model described in the Appendix of [15]. A square domain is discretized using a uniform square mesh and the tractions at each grid point are defined by the Lennard-Jones law of equation (8). The corresponding elastic deformations due to these tractions are determined by inversion of the elastic solution in Fourier space, which therefore implies periodic boundary conditions on the modelled domain. The combined [elastic + L-J] displacements at each point are required to satisfy the contact condition appropriate to a realization of the isotropic PSD (6). The resulting set of non-linear equations is satisfied using a damped molecular dynamic algorithm. For more details, the reader is referred to [15].

Since the numerical solution is based on a particular realization of equation (6), different results are obtained depending on the initial random number seed. In particular, the resulting force-displacement curve analogous to Fig. 4 is quite sensitive to the actual maximum height in the realization. This variability would of course be reduced if computational considerations allowed a larger region of the surface to be modelled. In Fig. 6, we compare the predictions of the present statistical algorithm with the average of four numerical realizations for the normalized mean traction $\bar{\sigma}/\sigma_0$, for three values of the height variance and $D = 2.2, \tilde{k}_1 = 1, \tilde{k}_2 = 8$.

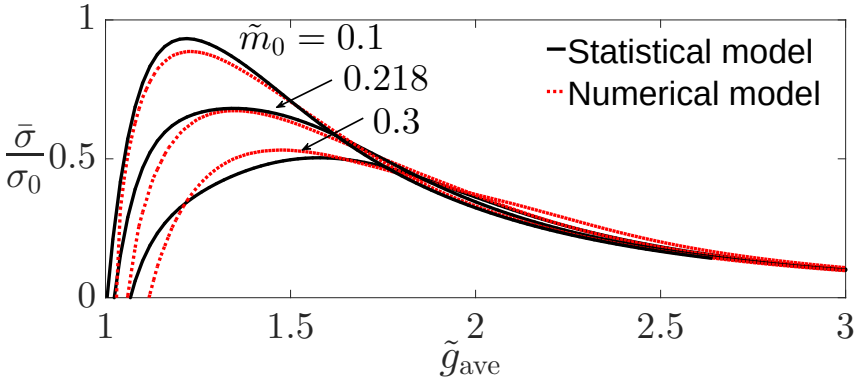

Fig. 6: Comparison of the predicted mean traction $\bar{\sigma}$ as a function of mean gap $\tilde{g}_{\text{ave}}$ using the present statistical method and the numerical method of [15]. Results are presented for $\tilde{k}_1 = 1, \tilde{k}_2 = 8, D = 2.2$ and three values of the dimensionless height variance $\tilde{m}_0 = m_0/\epsilon^2$.

6. A hybrid JKR theory

Many treatments of adhesive contact problems make use of the JKR formalism [12, 23, 24], since it is amenable to analytical solution, whereas a solution using the full Lennard-Jones traction law almost invariably requires numerical solution and even then the resulting problem can be quite challenging.

The present method opens up the possibility of decoupling the effect of fine-scale roughness [where the effective Tabor number is too small for the JKR approach to be reasonable], from coarse scale features. We first determine the reduced interfacial energy due to the fine-scale roughness $k > k_1$ using the methodology of Section 2. The rest of the profile, comprising roughness in the range $k < k_1$ and any macroscopic features of the contacting bodies can then be used to define a contact problem using the JKR formalism, but with $\Delta\gamma$ replaced by $\Delta\gamma_{\text{eff}}$.

7. Conclusions

We have described a procedure based on Persson's theory of rough surface contact for determining the effect of adding a small increment of the truncated PSD on the resulting probability distribution for the gap g, including contributions from elastic deformation and from the Lennard-Jones interfacial traction law. The L-J law is used throughout the compressive and tensile range and hence this theory does not include regions of 'hard' compressive contact where further variation of gap is impossible. As a result, the solution converges at large wavenumbers, in contrast to hard contact theories which generally require the PSD to be somewhat arbitrarily truncated.

Using this method, we are able to determine the effective reduction in interfacial energy and mean pull-off traction due to the fine scale [i.e. high wavenumber] components in the PSD. These results can then be used in problems formulated using the JKR formalism.

References

[1] Greenwood JA, Williamson JBP. The contact of nominally flat surfaces. Proc R Soc Lond 1966;A295:300–319.
doi: 10.1098/rspa.1966.0242

[2] Persson BNJ. Theory of rubber friction and contact mechanics. J Chem Phys 2001;115:3840–3861. doi: 10.1063/1.1388626

[3] Ciavarella M, Demelio G, Barber JR, Jang YH. Linear elastic contact of the Weierstrass profile. Proc R Soc Lond 2000;A456:387–405. doi: 10.1098/rspa.2000.0522

[4] Manners W, Greenwood JA. Some observations on Persson's diffusion theory of elastic contact. Wear 2006;261:600–610. doi:10.1016/j.wear.2006.01.007

[5] Pastewka L, Robbins MO. Contact between rough surfaces and a criterion for macroscopic adhesion. PNAS 2014;119:3298–3303. doi/10.1073/pnas.1320846111

[6] Bush AW, Gibson RD, Thomas TR. The elastic contact of a rough surface. Wear 1975;35:87–111. doi: 10.1016/0043-1648(75)90145-3

[7] Nayak PR.Random process model of rough surfaces, ASME J Lub Tech 1971;93(3):98–407. doi: 10.1115/1.3451608

[8] Aramaki H, Cheng HS, Chung Y-W. The contact between rough surfaces with longitudinal texture — Part I: Average contact pressure and real contact area, ASME J Tribol 1993;115:419–424. doi: 10.1115/1.2921653

[9] Greenwood JA, Wu JJ. Surface roughness and contact: an apology. Meccanica 2001;36:617–630. doi: 10.1023/A:1016340601964

[10] Borri-Brunetto M, Carpinteri A, Chiaia B. Lacunarity of the contact domain between elastic bodies with rough boundaries, in Probamat 97, Probabilities and Materials 1997. G. Frantziskonis, (ed.), Kluwer, Dordrecht.

[11] Gao YF, Bower AF. Elastic-plastic contact of a rough surface with Weierstrass profile. Proc R Soc Lond 2006;A462:319–348. doi: 10.1098/rspa.2005.1563

[12] Fuller KNG, Tabor D. The effect of surface roughness on the adhesion of elastic solids. Proc R Soc Lond 1975;A345:327–342. doi: 10.1098/rspa.1975.0138

[13] Johnson KL, Kendall K, Roberts AD. Surface energy and the contact of elastic solids. Proc R Soc Lond 1971;A324:301–313. doi: 10.1098/rspa.1971.0141

[14] Tabor D. Surface forces and surface interactions. J. Colloid Interface Sci 1977;58:2–13. doi: 10.1016/0021-9797(77)90366-6

[15] Persson BNJ, Scaraggi M. Theory of adhesion: Role of surface roughness. J Chem Phys 2014;141:124701. doi.org/10.1063/1.4895789

[16] Greenwood JA.On the DMT theory. Tribol Lett 2007;26:203–211. doi: 10.1007/s11249-006-9184-7

[17] Bradley RS. The cohesive force between solid surfaces and the surface energy of solids. Phil Mag 1932;13:853–862.

[18] Yu N, Polycarpou AA. Adhesive contact based on the LennardJones potential: a correction to the value of the equilibrium distance as used in the potential. J Colloid Interface Sci 2004;278:428–435.

[19] Gilman JJ. Direct measurements of the surface energies of crystals. J Appl Phys 1960;31:2208–2218.

[20] Beckmann P. Statistical distribution of the amplitude and phase of a multiply scattered field, J Res NBS 1962;D66:231–240.

[21] Almqvist A, Campaña C, Prodanov N, Persson BNJ. Interfacial separation between elastic solids with randomly rough surfaces: Comparison between theory and numerical techniques. J Mech Phys Solids 2011;59:2355–2369. doi:10.1016/j.jmps.2011.08.004

[22] Ciavarella M, Afferrante L. Adhesion of rigid rough contacts with bounded distribution of heights. Tribol Int 2016;100:18–23. doi: 10.1016/j.triboint.2015.10.033

[23] Johnson KL. The adhesion of two elastic bodies with slightly wavy surfaces. Int J Solids Struct 1995;32:423–430. doi: 10.1016/0020-7683(94)00111-9

[24] Guduru P. Detachment of a rigid solid from an elastic wavy surface: Theory. J Mech Phys Solids 2007;55:445–472. doi: 10.1016/j.jmps.2006.09.004